European Journal of Pharmacology 641 (2010) 199–206

Contents lists available at ScienceDirect

European Journal of Pharmacology

journal homepage: www.elsevier.com/locate/ejphar

Cardiovascular Pharmacology

Epigallocatechin gallate protects H9c2 cardiomyoblasts against hydrogen dioxides-induced apoptosis and telomere attrition

Rui Sheng [a,b], Zhen-lun Gu [a,b,*], Mei-lin Xie [a], Wen-xuan Zhou [a], Ci-yi Guo [a]

[a] Suzhou Institute of Chinese Meteria Medica, Department of Pharmacology, Medical School of Suzhou University, 215123 Suzhou, China
[b] Laboratory of Aging and Nervous Diseases, Department of Pharmacology, Medical School of Suzhou University, 215123 Suzhou, China

ARTICLE INFO

Article history:
Received 24 October 2009
Received in revised form 8 May 2010
Accepted 31 May 2010
Available online 8 June 2010

Keywords:
EGCG
Oxidative stress
H9c2 cardiomyoblasts
Apoptosis
Telomere
TRF_2
p53

ABSTRACT

Epigallocatechin gallate (EGCG), the major component of polyphenols in green tea, has recently attracted considerable attention for its cardioprotective effects. Telomere signalling plays a role in regulating cardiomyocyte apoptosis during cardiac dysfunction. The purpose of this study was to investigate the effects of EGCG on oxidative stress-induced apoptosis and telomere attrition in cardiomyocytes. H9c2 cells were incubated with EGCG, 50 and 100 mg/l, for 24 h. Apoptosis induced by 200 μmol/l hydrogen dioxide (H_2O_2) was analyzed by DAPI nuclear staining, electron microscopy, electrophoresis of DNA fragments and flow cytometry. When H9c2 cells were incubated with H_2O_2 for 12–24 h, the intracellular and extracellular H_2O_2 concentrations were not affected by the presence of EGCG. Chromatin condensation, DNA fragmentation and apoptotic body formation were observed in H_2O_2-induced injury. Flow cytometry analysis showed that the apoptotic rate increased remarkably. EGCG significantly inhibited H_2O_2-induced apoptotic morphological changes and apoptotic rate. When H9c2 cells were incubated with H_2O_2, the telomere length shortened and the protein expression of telomere repeat-binding factor 2 (TRF_2) decreased gradually, while the protein levels of p53 and p21 increased. EGCG significantly inhibited telomere attrition, TRF_2 loss and p53, p21 upregulation induced by H_2O_2. These results suggested that EGCG might suppress oxidative stress-induced cardiomyocyte apoptosis through inhibiting telomere dependent apoptotic pathway.

1. Introduction

It was proposed that chronic, low levels of cardiomyocyte apoptosis might be a critical factor during the transition from cardiac hypertrophy or myocardial infarction to heart failure (Li et al., 1997; Kang and Izumo, 2000; Wencker et al., 2003). However, our understanding of potential strategies to prevent cardiomyocyte apoptosis and senescence is limited. On the cellular level, senescence, chromosome stability, cell viability and apoptosis are regulated by the telomeres and their associated proteins, located at both ends of eukaryotic chromosomes (Blasco, 2005). Telomeres consist of tandem T2AG3 repeats at chromosome ends, maintained by telomerase reverse transcriptase (TERT), and bound by specific telomere repeat-binding factors (TRFs) including TRF_1 and TRF_2 (de Lange, 2002; Blackburn, 2001; McEachern et al., 2000; van Steensel et al., 1998). In addition to the protection of chromosome ends, the components of the telomeric complex could regulate cell survival and death. Some gene products implicated in growth arrest and apoptosis, such as p53 and p21, are potential downstream effectors of the telomeric complex and increase with age in cardiomyocytes (Chin et al., 1999; Leri et al., 2003; Sano et al., 2007). Recent evidence showed that telomere signalling plays a role in regulating adult cardiomyocyte apoptosis during cardiac dysfunction (Oh et al., 2003). Telomere attrition was also found during the pathogenesis of myocardial infarction and senesce (Fuster and Andres, 2006). However, little is known about drug effects on telomere attrition dependent apoptotic pathway in oxidative stress-induced cardiomyocyte injury.

Epigallocatechin gallate (EGCG), the major component of polyphenols in green tea, has recently attracted considerable attention for its antioxidative, anti-inflammatory, antitumorigenic and antisenescent properties (Higdon and Frei, 2003). Recent studies have demonstrated the protective effects of EGCG and green tea on cardiovascular diseases (Chyu et al., 2004; Priyadarshi et al., 2003). Townsend et al. (2004) reported that green tea extracts and EGCG protect cardiomyocytes against ischemia/reperfusion-induced apoptotic cell death both in vivo and in vitro. More recently, Yao et al. (2008) found that EGCG protected human lens epithelial cells from the mitochondria-mediated apoptosis induced by hydrogen peroxide (H_2O_2). In the previous study, we found that EGCG inhibited cardiomyocyte apoptosis and oxidative stress in pressure overload-induced cardiac hypertrophy (Sheng et al., 2007,

* Corresponding author. Suzhou Institute of Chinese Meteria Medica, Department of Pharmacology, Medical School of Suzhou University, 215123 Suzhou, China. Tel./fax: +86 512 6519 0599.
E-mail addresses: sheng_rui@163.com (R. Sheng), zhenlungu.2003@163.com (Z. Gu).

0014-2999/$ – see front matter © 2010 Elsevier B.V. All rights reserved.
doi:10.1016/j.ejphar.2010.05.054

2009). It has been demonstrated that oxidative stress induces telomere DNA injury, promotes telomere attrition, and leads to cell senescence and apoptosis in human vascular endothelial cells and Hela cells. Furthermore, several antioxidants such as ascorbic acid, N-acetyl-L-cysteine, glutathione and atorvastatin have been found to prevent telomere shortening (Ben-Porath and Weinberg, 2004; Duan et al., 2005; Furumoto et al., 1998; Mahmoudi et al., 2008; Ren et al., 2001; Voghel et al., 2008). Thus, we hypothesize that the antiapoptotic effect of EGCG in cardiomyocytes is partly mediated by telomere dependent apoptotic pathway.

In this study, the H9c2 cardiomyoblasts were treated with H_2O_2 to establish an oxidative stress-induced apoptosis model. The effects of EGCG on oxidative stress-induced apoptosis and telomere dependent apoptotic pathway in H9c2 cells were investigated.

2. Materials and methods

2.1. Cell culture and drug treatment

The rat embryonic, heart derived cardiomyoblast cell line, H9c2 (ATCC, Rockville, MD, USA), was cultured in Dulbecco modified Eagle medium (DMEM, GIBCO, Carlsbad, CA, USA), containing 1.5 g/l sodium bicarbonate and 4.5 g/l glucose, supplemented with 10% fetal bovine serum. To prevent the loss of myoblastic cells, cells were subcultured before confluence (Hescheler et al., 1991; L'Ecuyer et al., 2004; Winstead et al., 2005). Before subculturing, the cells were counted using a hemocytometer and population doubling (PD) levels were calculated. In the preliminary study, telomeres in H9c2 cells shortened by 0.1–0.2 kb per passage on average during serial subcultivation, which were in accordance with the results of Furumoto et al. (1998). In the present study, exponentially growing cells from passages 20 ± 2 were used for subsequent experiments.

The cells were treated with H_2O_2 and EGCG for the indicated time periods. After pretreatment with EGCG (Sigma, St Louis, USA, purity $\geq$ 95%) at concentrations of 50 and 100 mg/l for 24 h, 200 μmol/l H_2O_2 was added and incubated with the cells for an additional 24 h. The cells in control group were treated with the same volume of phosphate-buffered saline (PBS), while the cells in model groups were incubated with H_2O_2 at 200 μmol/l for 3–24 h. The morphological changes of cells were observed using a phase contrast microscope.

2.2. Extracellular and intracellular hydrogen peroxide measurement

The cells were incubated with EGCG and H_2O_2 at the indicated concentration and period, and then the culture media were harvested to determine the extracellular H_2O_2 concentration. Afterwards, the cells were lysed in 100 μl lysis buffer supplied by the H_2O_2 assay kit (Beyotime Institute of Biotechnology, China). The supernatants, gathered by centrifuging at 12,000 × *g* for 10 min, were used to determine the intracellular H_2O_2 concentration. The intracellular and extracellular H_2O_2 concentrations were measured with the assay kit according to the manufacturer's instructions (Dai et al., 2007). In brief, sample solution (50 μl) was incubated with reaction solution (100 μl) at room temperature for 30 min, and then the absorption at 560 nm was measured. The H_2O_2 concentration was calculated by the standard curve made from the standard solutions.

2.3. DAPI nuclear staining

Chromatin condensation was assessed by staining cells with 4, 6-diamidino-2-phenylindole (DAPI, Molecular probes, Eugene, OR, USA). The cells were fixed in 4% paraformaldehyde–PBS solution for 15 min and stained with DAPI 300 nmol/l for 30 min at room temperature. Then nuclear morphology was visualized by fluorescence microscopy. Apoptotic cells were recognized by the condensed, fragmented, and degraded nuclei (Ogata et al., 2003).

2.4. Agarose gel electrophoresis for DNA fragmentation

Cellular genomic DNA was isolated and electrophoresed on 2% agarose gel using the method described previously with minor modification (Aikawa et al., 2000). In brief, the cells were lysed in 0.6 ml of lysis buffer containing 100 mmol/l NaCl, 25 mmol/l EDTA, 10 mmol/l Tris–HCl (pH 8.0), 0.5% SDS, and 66.7 mg/l RNase A at 55 °C for 2 h. Incubation was continued overnight after adding 1 mg/ml protease K. DNA was extracted with phenol: chloroform: isoamyl alcohol (24:25:1). DNA fragments were separated on 2% agarose gel, detected with a UV transluminator after staining with ethidium bromide, and visualized by Gel Document 2000 (Bio-Rad, Hercules, CA, USA).

2.5. Flow cytometry analysis

The cells ($>10^6$) were digested with 0.25% trypsin and collected by centrifugation. After washing twice with ice-cold PBS, the cells were fixed in ice-cold 70% ethanol. After centrifugation, the fixed cells were incubated with RNase 100 mg/l at 37 °C for 30 min and stained with 50 mg/l propidium iodide (PI) for 30 min. The cells were analyzed by EPICS XL flow cytometry (Beckman Coutler, CA, USA). The hypodiploid population of cells was considered apoptotic, and the apoptotic rate was analyzed by Multicycle software (Beckman Coutler, CA, USA).

2.6. Transmission electron microscopic examination

The cells were harvested and fixed in ice-cold 2.5% glutaraldehyde for 4 h at 4 °C. Then the cells were post-fixed in 1% osmium tetroxide, dehydrated in graded alcohols, embedded in Epon 812, sectioned with an ultra-microtome, and stained with uranyl acetate and lead citrate followed by examination with a transmission electron microscope (H-600, Hitachi, Japan).

2.7. Telomere length measurement

Telomere length was determined by a Telomere Length Assay kit (Roche Diagnostics, Mannheim, Germany). The cells were harvested and genomic DNA was isolated as described by the assay kit protocol. 2 μg purified DNA was digested with 20 U each of *Hin*fI and *Rsa*I at 37 °C for 4 h. The DNA fragments were separated on 0.8% agarose and transferred to positive charged nylon membranes (Amersham, Arlington Height, IL, USA) by capillary transfer using 20× SSC transfer buffer (3 mol/l NaCl, 0.3 mol/l trisodium citrate). The blotted DNA fragments were hybridized to a digoxigenin-labeled probe specific for telomeric repeats and incubated with a digoxigenin-specific antibody covalently coupled to alkaline phosphate. Finally, the immobilized telomere probe was visualized by virtue of alkaline phosphatase metabolizing CDP-Star, a highly sensitive chemiluminescence substrate. The average telomere length was determined by comparing the signals relative to a molecular weight standard with CALCTRF software. (Ball and Levine, 2005)

2.8. Western blot analysis

The cells were washed twice with ice-cold PBS and lysed in a buffer containing Tris–HCl (pH 7.4) 10 mmol/l, NaCl 150 mmol/l, 1% Triton X-100, 1% sodium deoxycholate, 0.1% SDS, edetic acid 5 mmol/l, phenylmethylsulfonyl fluoride (PMSF) 1 mmol/l, aprotinin 0.28 kU/l, leupeptin 50 mg/l, benzamidine 1 mmol/l, and pepstatin A 7 mg/l. Protein concentration was determined by a bicinchoninic acid (BCA) kit (Pierce, Rockford, IL, USA). 50 μg of protein from each sample was loaded onto 12% SDS-PAGE gel and subjected to electrophoresis. The

proteins were transferred to nitrocellulose membranes (Amersham, Arlington Height, IL, USA) and incubated with rabbit anti-TRF_2 polyclonal antibody (1: 200; sc-9143, Santa Cruz, CA, USA), mouse anti-p53 monoclonal antibody (1:200; sc-100) or mouse anti-p21 monoclonal antibody (1: 200; sc-6246) for 3 h. The membranes were then washed and incubated with horseradish peroxidase-conjugated secondary antibody for another 1 h. Immunoreactivity was detected by enhanced chemoluminescent autoradiography. The results were analyzed quantitatively using SigmaScan Pro 5.0.0. The data were normalized with respect to the ratios of actin detected on the same blot (Planavila et al., 2005; Sheng et al., 2007) .

2.9. Statistical analysis

SPSS 10.0 software (SPSS Inc, Chicago, Illinois, USA) was used for the statistical analysis. For the comparison of nominal data, one-way ANOVA was used and the intergroup comparisons (post-hoc analysis) among the data with equal variances were made by the Bonferroni method to employ correction for multiple comparisons with the post hoc analysis, while Tamhane's T2 method was used for the data with unequal variances. Nonparametric tests were used for data without normal distribution. The Mann–Whitney *U* tests were used to compare groups according to the group number.

3. Results

3.1. EGCG has no effects on H_2O_2 concentration in H9c2 cells

When the H9c2 cells were exposed to H_2O_2 at 200 μmol/l for 12 h and 24 h, the extracellular and intracellular H_2O_2 concentration significantly increased. However, the H_2O_2 concentration in culture medium was not affected by the presence of EGCG (Fig. 1, $P>0.05$). Furthermore, addition of EGCG did not affect intracellular H_2O_2 concentration, either ($P>0.05$).

3.2. EGCG inhibits H_2O_2 induced apoptosis in H9c2 cells

When the H9c2 cells were exposed to 200 μmol/l H_2O_2 for 12 h and 24 h, the sizes of most cells reduced obviously. Cytoplasm shrinkage and nuclei pyknosis were found by phase contrast microscopy (Fig. 2A). When the cells were stained with the DNA-binding dye DAPI, the cells revealed condensed chromatin, fragmented nuclei and formation of apoptotic bodies, which are characteristics of apoptosis (Fig. 2B). Using transmission electron microscopy, we observed many cells showing apoptotic ultramicrostructures such as cytoplasm shrinkage, slight swelling of endoplasmic reticulum and chromatin condensation against the inner surface of the nuclear membrane (Fig. 2C). Pretreatment with EGCG 50 and 100 mg/l for 24 h significantly attenuated the morphological changes in H9c2 cells as shown in Fig. 2A–C. When apoptotic rate was quantified by flow cytometry (FCM), the apoptotic cells increased from 0% in the control group to 16.4% in the H_2O_2 24 h group ($P<0.01$ vs. the control group; Fig. 2D, E). Pretreatment with EGCG 50 and 100 mg/l for 24 h decreased the apoptotic rate to 3.7% and 2.9%, respectively ($P<0.01$ vs. the H_2O_2 24 h group). The percentage of apoptotic cells (i.e. the percentage of cells in the sub-G1 fraction) was similar to the apoptotic population measured by DAPI (data not shown). The level of DNA fragmentation was further analyzed by gel electrophoresis. The H9c2 cells incubated with H_2O_2 showed increased fragmentation of lower molecular weight DNAs, whereas EGCG significantly decreased the DNA fragmentation (Fig. 2F).

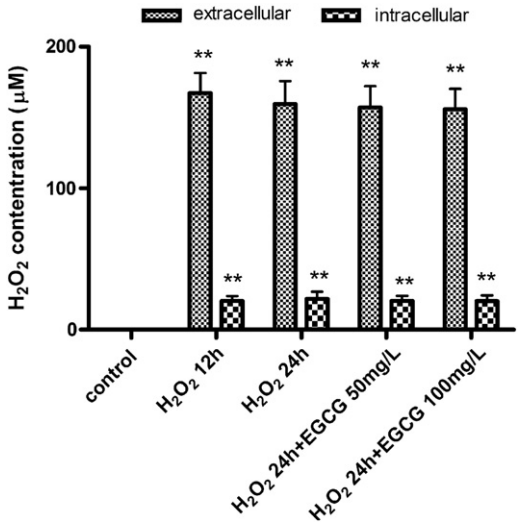

Fig. 1. Effects of EGCG on H_2O_2 concentration in H9c2 cells. H9c2 cells were preincubated with EGCG at 50 and 100 mg/l for 24 h. H9c2 cells were incubated with 200 μmol/l H_2O_2 for 12 and 24 h. The extracellular and intracellular H_2O_2 were determined by chemical colorimetry. Mean ± S.D., $n=6$, $^{**}P<0.01$ vs. control group.

3.3. EGCG inhibits H_2O_2 induced telomere attrition in H9c2 cells

In control H9c2 cells, the telomere length was 21.1 ± 1.0 kb. When the cells were incubated with 200 μmol/l H_2O_2 for 12 h, the telomere length was 19.3 ± 0.7 kb, showing a shortening tendency though with no significance ($P>0.05$). When the cells were incubated with 200 μmol/l H_2O_2 for 24 h, the telomere length significantly shortened (17.6 ± 0.6 kb, $P<0.05$ vs. control group), suggesting that H_2O_2 induces telomere attrition in H9c2 cells. However, preincubation with EGCG at 50 and 100 mg/l for 24 h significantly protected H9c2 cells from H_2O_2-induced telomere attrition and maintained the telomere length at 18.4 ± 0.4 kb and 19.6 ± 0.3 kb ($P<0.05$ vs. H_2O_2 24 h group, Fig. 3).

3.4. EGCG inhibits H_2O_2 induced TRF_2 loss in H9c2 cells

When H9c2 cells were treated with 200 μmol/l H_2O_2 for 3–24 h, the protein expression of TRF_2 gradually decreased with time. The protein levels of TRF_2 at 3 h, 6 h, 12 h and 24 h after H_2O_2 treatment were 40.36%, 36.4%, 26.0% and 9.7% of that of control group, respectively ($P<0.05$ or $P<0.01$ vs. control group, Fig. 4), suggesting that H_2O_2 significantly downregulates TRF_2 expression in H9c2 cells. When the cells were pretreated with 50, 100 mg/l of EGCG for 24 h, the protein levels of TRF_2 returned to 61.7% and 72.5% of that of control group ($P<0.05$ or $P<0.01$ vs. H_2O_2 24 h group), suggesting that EGCG significantly recovered the expression of TRF_2.

3.5. EGCG prevents H_2O_2 induced p53 upregulation in H9c2 cells

When H9c2 cells were treated with 200 μmol/l H_2O_2 for 3–24 h, the expression of p53 protein progressively increased and reached maximum levels at 24 h. The protein levels of p53 at 3 h, 6 h, 12 h and 24 h after H_2O_2 treatment were 1.6, 2.7, 2.9 and 3.8 times of that of control group, respectively ($P<0.05$ or $P<0.01$ vs. control group, Fig. 5), suggesting that H_2O_2 induces upregulation of p53 protein in H9c2 cells. EGCG, at doses of 50 and 100 mg/l, significantly prevented p53 upregulation induced by H_2O_2. The protein levels of p53 were reduced to 61.3% and 54.6% of that of H_2O_2 24 h group ($P<0.05$ vs. H_2O_2 24 h group).

3.6. EGCG prevents H_2O_2 induced p21 upregulation in H9c2 cells

When H9c2 cells were treated with 200 μmol/l H_2O_2 for 3–24 h, the p21 protein expression progressively increased and reached maximum at 24 h. The protein levels of p21 at 3 h, 6 h, 12 h and 24 h

after H_2O_2 treatment reached 1.6, 2.9, 3.4 and 4.2 times of that of control group, respectively ($P<0.05$ or $P<0.01$ vs. control group, Fig. 6), suggesting that H_2O_2 upregulates p21 protein in H9c2 cells. EGCG, at doses of 50 and 100 mg/l, significantly prevented H_2O_2-induced p21 upregulation. The protein levels of p21 were 53.1% and 29.2% of that of H_2O_2 24 h group ($P<0.01$ vs. H_2O_2 24 h group).

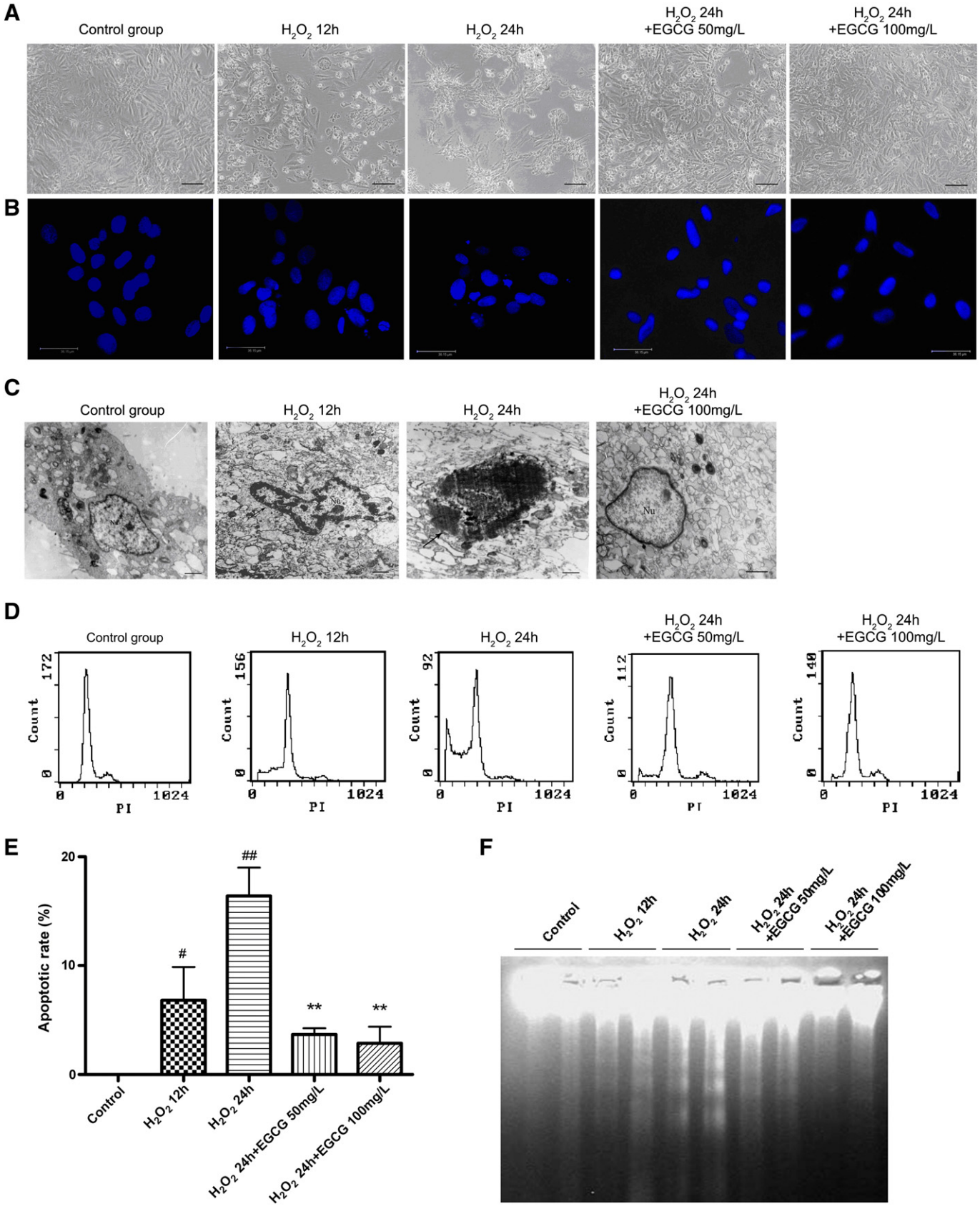

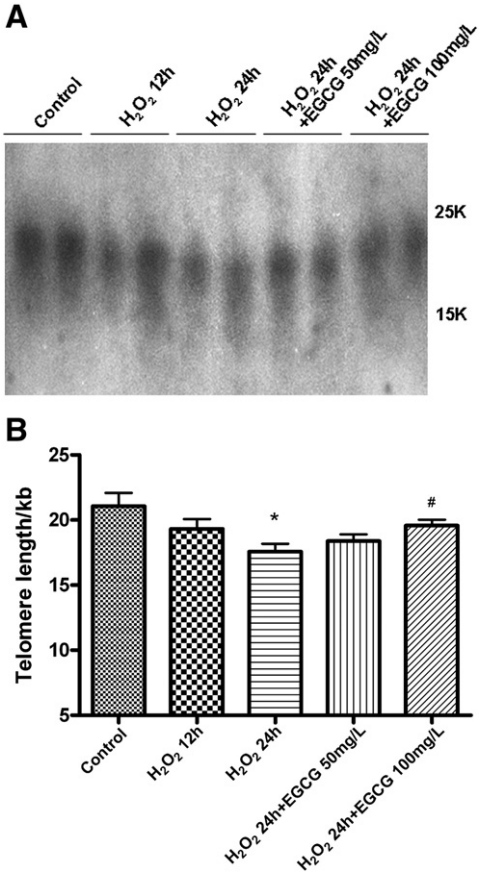

Fig. 3. EGCG inhibits H_2O_2 induced telomere attrition in H9c2 cells. H9c2 cells were treated as described in the legend of Fig. 2. Genomic DNA was extracted from cell lysates and telomere length was measured by southern blot analysis. (A) Representative southern blot results showing telomere length in H9c2 cells. (B) Quantitative analysis of telomere length in H9c2 cells. Mean ± S.D., $n=3$, $^{*}P<0.05$ vs. control group, $\#P<0.05$ vs. H_2O_2 24 h group.

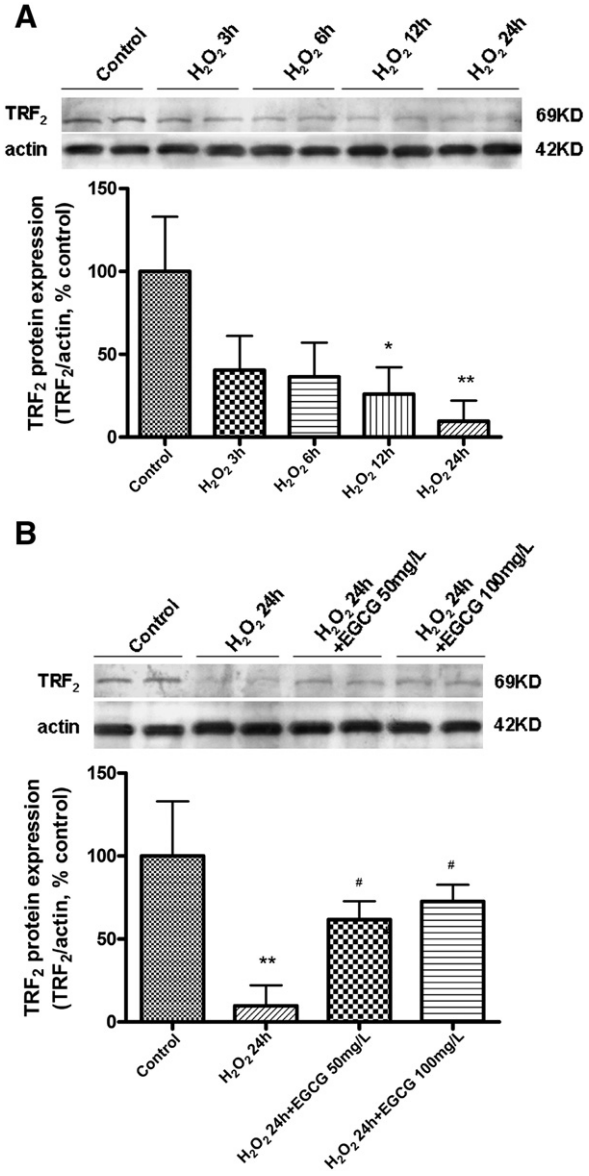

Fig. 4. Effects of EGCG on TRF_2 protein expression in H_2O_2-induced H9c2 cell injury. (A) Time-dependent changes of TRF_2 protein expression in H_2O_2-induced H9c2 cell injury. H9c2 cells were incubated with for 3, 6, 12 and 24 h. (B) EGCG inhibits H_2O_2-induced TRF_2 loss in H9c2 cells. H9c2 cells were preincubated with EGCG at 50 and 100 mg/l for 24 h. Cells were incubated with 200 μmol/l H_2O_2 for additional 24 h. Protein levels of TRF_2 in H9c2 cells were determined by western blot analysis. Levels of α-actin protein were used as the loading control. Quantitative analysis was performed with Sigma Pro 5. Mean ± S.D., $n=3$, $^{*}P<0.05$, $^{**}P<0.01$ vs. control group, $\#P<0.05$, $\#\#P<0.01$ vs. H_2O_2 24 h group.

4. Discussion

H9c2 is a rat-derived cardiomyoblast cell line that has been used to investigate heart function (Hescheler et al., 1991; L'Ecuyer et al., 2004). H9c2 cells exhibit morphological characteristics similar to those of immature embryonic cardiomyocytes but preserve several elements of the electrical and hormonal signal pathway found in adult cardiac cells. Evidences showed that H_2O_2 induces the same oxidative stress in H9c2 cells as in primary cultured rat cardiomyocytes (Winstead et al., 2005). Therefore, this cell line may be useful as a model for oxidative stress-induced cardiomyocyte injury in aspects of transmembrane signal transduction. In previous study, we found that EGCG inhibited apoptosis induced by oxidative stress in primary cultured rat cardiomyocytes, which prompted us to examine the effects of EGCG on H_2O_2 induced apoptosis in H9c2 cardiomyoblasts. In this study, apoptosis in H9c2 cells was induced by 200 μmol/l H_2O_2 and the effects of EGCG on apoptosis, telomere length and TRF_2, p53 and p21 expression were examined. The results showed that EGCG pretreatment significantly suppressed H_2O_2-induced apoptotic morphological changes and reduced the apoptotic rate. When H9c2 cells were incubated with H_2O_2, progressive telomere attrition and TRF_2 protein reduction were detected, while p53 and p21 protein levels were upregulated gradually. EGCG pretreatment greatly prevented telomere attrition, and inhibited TRF_2 loss and p53, p21 upregulation induced by oxidative stress.

H_2O_2, one major kind of reactive oxygen species (ROS), can lead to the formation of hydroxyl radicals (·OH) mediated by intracellular

Fig. 2. EGCG inhibits H_2O_2-induced apoptosis in H9c2 cells. H9c2 cells were preincubated with EGCG at 50 and 100 mg/l for 24 h. H9c2 cells were incubated with 200 μmol/l H_2O_2 for 12 and 24 h. (A) Effects of EGCG on H_2O_2-induced morphological changes in H9c2 cells. Cell morphological changes were observed by phase contrast microscopy. Bar = 200μm. (B) Effects of EGCG on DAPI nuclear staining in H_2O_2-induced H9c2 cell injury. DAPI nuclear staining was observed under fluorescence microscopy. Bar = 36 μm. (C) Effects of EGCG on H_2O_2-induced ultrastructural morphological changes in cultured H9c2 cells. Ultrastructural morphology of H9c2 cells was detected by transmission electron microscopy. Arrows indicate chromatin condensation. Nu: nucleus. Bar = 2μm (D) Effects of EGCG on H_2O_2-induced apoptotic peak in H9c2 cells. Cells were fixed in ethanol and stained with PI. Hypodiploid apoptotic peak was detected by flow cytometry. (E) Quantitative analysis of the apoptotic rate in flow cytometry. Mean ± S.D., $n=3$, $^{**}P<0.01$ vs. control group, $^{\#\#}P<0.01$ vs. H_2O_2 24 h group. (F) Effects of EGCG on H_2O_2-induced DNA fragmentation in H9c2 cells. Genomic DNA was extracted from cell lysates and electrophoresed on 2% agarose gel.

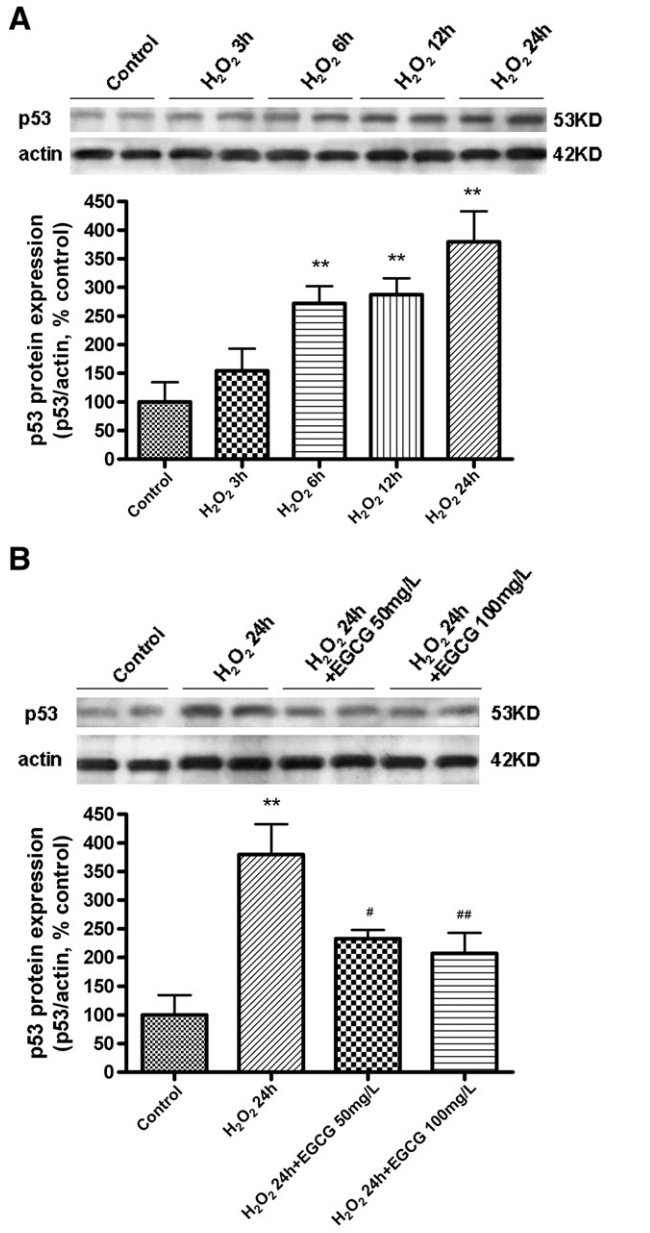

Fig. 5. Effects of EGCG on p53 protein expression in H_2O_2-induced H9c2 cell injury. H9c2 cells were treated as described in the legend of Fig. 4. (A) Time-dependent changes of p53 protein expression in H_2O_2-induced H9c2 cell injury. (B) EGCG inhibits H_2O_2-induced p53 upregulation in H9c2 cells. Mean ± S.D., $n = 3$, $^{*}P<0.05$, $^{**}P<0.01$ vs. control group, #$P<0.05$, ##$P<0.01$ vs. H_2O_2 24 h group.

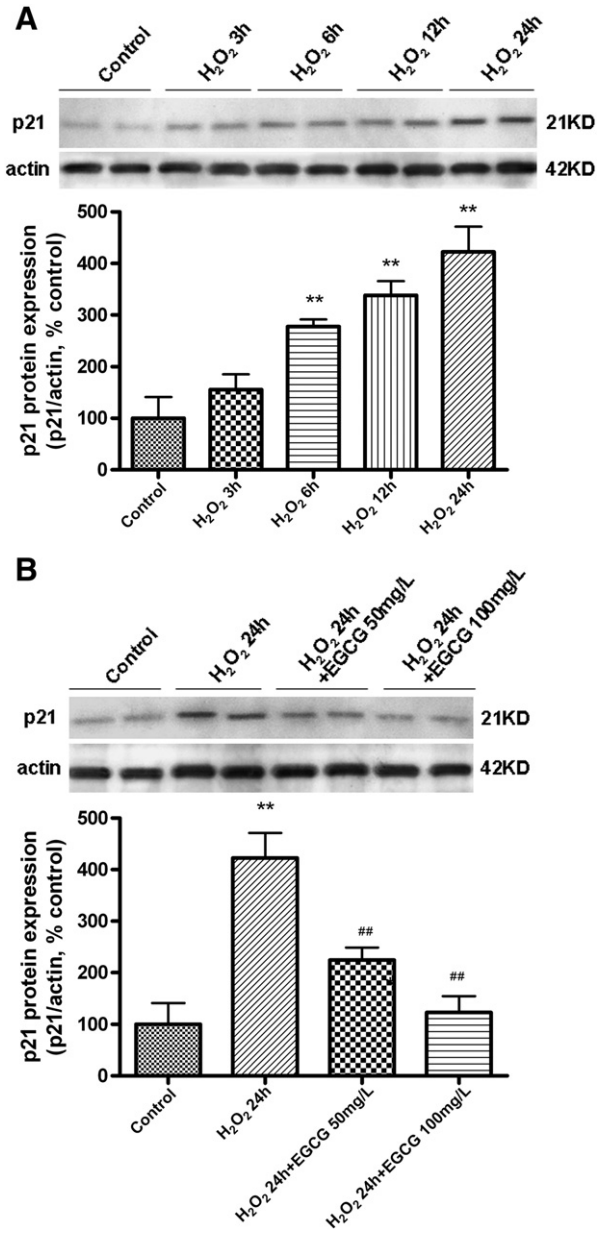

Fig. 6. Effects of EGCG on p21 protein expression in H_2O_2-induced H9c2 cell injury. H9c2 cells were treated as described in the legend of Fig. 4. (A) Time-dependent changes of p21 protein expression in H_2O_2-induced H9c2 cell injury. (B) EGCG inhibits H_2O_2-induced p21 upregulation in H9c2 cells. Mean ± S.D., $n = 3$, $^{*}P<0.05$, $^{**}P<0.01$ vs. control group, #$P<0.05$, ##$P<0.01$ vs. H_2O_2 24 h group.

heavy metal ions through the Fenton reaction. Many studies have demonstrated that EGCG might reduce H_2O_2 concentration to exert beneficial antioxidative activity. Hung's group found that EGCG inhibits ultraviolet (UV) radiation-induced H_2O_2 production in human retinal pigment epithelium cells and keratinocyte (Chan et al., 2008; Wu et al., 2006). EGCG also decreased intracellular H_2O_2 level in stromal fibroblasts (Hung et al., 2005). Conversely, some recent reports demonstrated that EGCG could produce H_2O_2 to exert bactericidal actions or activate pancreatic beta cell damages (Arakawa et al., 2004; Suh et al., 2009). Accordingly, the effects of EGCG on H_2O_2 concentration may be altered according to the cellular environments and characteristics of the particular cell line investigated. In this study, to rule out the possibility that EGCG cancels the effect of H_2O_2 by a direct chemical interaction, we measured the extracellular and intracellular H_2O_2 concentration in H9c2 cells. Our results showed that H_2O_2 concentration in culture medium was not affected by the presence of EGCG. Furthermore, addition of EGCG did not affect intracellular H_2O_2 concentration, either. Therefore, the protective effects of EGCG against H_2O_2-induced injury should not be a direct chemical-neutralizing effect on H_2O_2.

Both H_2O_2 and OH induce severe intracellular oxidant stress, which damages various intracellular biomacromolecules and eventually results in apoptosis and necrosis of cells (Harsdorf et al., 1999). The representative characteristics of apoptosis include chromatic condensation, DNA fragmentation and the formation of apoptotic body, etc (Adams, 2003; van Empel et al., 2005). The methods frequently used to detect apoptosis include DNA fragment gel electrophoresis, flow cytometry and electron microscopy, etc (Hunter et al., 2005; Peter et al., 1997). In this study, DAPI nuclear staining, electron microscopy, and DNA fragment gel electrophoresis were used to analyze the apoptotic morphology of H9c2 cells. Flow cytometry was used to quantitatively evaluate the apoptotic rate in H9c2 cells. The results

showed that H_2O_2 induced condensed chromatin, fragmented nuclei and formation of apoptotic bodies in H9c2 cells, which are characteristics of apoptosis. Preincubation with EGCG at 50 and 100 mg/l for 24 h significantly improved the morphological changes and reduced the apoptotic rate in H9c2 cells, suggesting that EGCG effectively inhibits oxidative stress-induced apoptosis in H9c2 cells.

The telomeres, especially the cascade structures abundant with base G repeats, are more sensitive to oxidative stress than the other genomic fragments. Oxidative stress induced by H_2O_2 or ·OH may directly oxygenize the base G and damage the telomere, lead to telomere disruption and attrition, and hence result in cellular apoptosis and senescence (Ben-Porath and Weinberg, 2004; Duan et al., 2005; Henle et al., 1999; Oikawa and Kawanishi, 1999). Furthermore, several antioxidants such as vitamin C, N-acetyl-L-cysteine, glutathione and atorvastatin have been found to prevent telomere shortening and apoptosis from oxidative stress in human vascular endothelial cells and Hela cells (Furumoto et al., 1998; Mahmoudi et al., 2008; Ren et al., 2001; Voghel et al., 2008). It is known that EGCG has an exceptional antioxidant capacity, even far exceeding than that of vitamin E and vitamin C (Rice-Evans, 1999). Thus, we assumed that the anti-apoptotic effect of EGCG may be related to its antioxidant effects by preventing telomere shortening. In this study, when H9c2 cells were treated with 200 μmol/l H_2O_2 for 24 h, the telomere length shortened significantly compared with that of control group, whereas EGCG at 50 and 100 mg/l significantly suppressed H_2O_2-induced telomere attrition. This result suggests that oxidative stress accelerates telomere shortening and induces cell apoptosis in H9c2 cells, while EGCG, with potent antioxidant effect, might inhibit apoptosis by preventing telomere shortening.

The telomere length is regulated by telomerase and telomere repeat-binding factor 2 (TRF_2). In our preliminary study, we first detected telomerase reverse transcriptase (TERT) mRNA expression by *in situ* hybridization. However, although TERT expression was present in control and H_2O_2-treated H9c2 cells, no significant alteration of TERT mRNA was found till 24 h after H_2O_2 treatment (data not shown), suggesting a mechanism other than defective telomerase activity for telomere attrition after oxidative stress. To test an alternative mechanism for telomere dysfunction, TRF_2 expression was further examined in the present study. TRF_2 can bind to the TTAGGG repeats of telomeres and contributes to the formation of the chromosome-protecting T-loops. A decrease in TRF_2 is thought to be the rate-limiting step for some forms of apoptosis (Blackburn, 2001; Griffith et al., 1999; Multani et al., 2000; van Steensel et al., 1998). Oh et al. (2003) reported that interference with either TRF_2 function or expression triggered telomere erosion and apoptosis in cultured cardiomyocytes. Conversely, exogenous TRF_2 conferred protection from oxidative stress. In circulating progenitor cells, TRF_2 was identified as a regulator of clonogenic potential and migratory capacity that can be modified by pharmacological treatment (Gensch et al., 2007; Spyridopoulos et al., 2004). More recently, Werner et al. (2008) further reported that voluntary physical exercise up-regulates cardiac TRF_2, and thereby induces anti-senescent effects, to prevent doxorubicin-induced apoptosis in cardiomyocytes. In this study, the results of western blot analysis showed a progressive downregulation of TRF_2 when H9c2 cells were treated with H_2O_2 for 3–24 h, but pretreatment with EGCG at 50 and 100 mg/l for 24 h significantly suppressed oxidative stress-induced TRF_2 loss in H9c2 cells. The results suggest that oxidative stress represents a potent regulator of the telomere length by affecting TRF_2 expression, and EGCG maintains the telomere length by preventing TRF_2 loss.

Several gene products implicated in growth arrest and apoptosis, such as p53 and p21, are potential downstream effectors of the telomeric complex and increase with age and oxidative stress in cardiomyocytes. Evidences showed that the tumor suppressor protein p53 could mediate telomere dysfunction (Leri et al., 2003; Sano et al., 2007). p53 was recently identified as a key mediator of maladaptive cardiac remodeling essential for the transition from cardiac hypertrophy to heart failure (Sano et al., 2007). Importantly, p53 may modulate apoptosis and senescence by increasing the expression of specific proteins, including Bax, Bad, and p21, etc. In addition, knockout of TRF_2 expression not only induces progressive telomere erosion, but also activates proapoptotic mediators p53 and p21, resulting in cell cycle arrest and initiating cell apoptosis (Chandel et al., 2000; Johnson et al., 1996; Kemp et al., 2003; Trinei et al., 2002). In this study, when the H9c2 cells were treated with 200 μmol/l H_2O_2 for 3–24 h, the p53 and p21 protein expression gradually increased and reached maximum at 24 h, while EGCG at doses of 50 and 100 mg/l significantly inhibits H_2O_2-induced p53 and p21 protein upregulation. These results suggest that EGCG might protect H9c2 cells against apoptosis via regulating p53 and p21, the downstream effectors of the telomeric complex.

5. Conclusion

In summary, this report provides evidence showing that cardiomyocyte apoptosis induced by oxidative stress is partly mediated by telomere dependent apoptotic pathway. EGCG, with potent antioxidant effect, attenuates oxidative stress-induced cardiomyocyte apoptosis through inhibiting telomere attrition-mediated apoptotic pathway.

Acknowledgements

This work was supported by grants from the Natural Science Foundation of China (30801391, 30930035), the Natural Science Foundation of Jiangsu Province (BK 2007548).

References

Adams, J.M., 2003. Ways of dying: multiple pathways to apoptosis. Genes Dev. 17, 2481–2495.
Aikawa, R., Nawano, M., Gu, Y., Katagiri, H., Asano, T., Zhu, W., Nagai, R., Komuro, I., 2000. Insulin prevents cardiomyocytes from oxidative stress-induced apoptosis through activation of PI3 kinase/ Akt. Circulation 102, 2873–2879.
Arakawa, H., Maeda, M., Okubo, S., Shimamura, T., 2004. Role of hydrogen peroxide in bactericidal action of catechin. Biol. Pharm. Bull. 27, 277–281.
Ball, A.J., Levine, F., 2005. Telomere-independent cellular senescence in human fetal cardiomyocytes. Aging Cell 4, 21–30.
Ben-Porath, I., Weinberg, R.A., 2004. When cells get stressed: an integrative view of cellular senescence. J. Clin. Invest. 113, 8–13.
Blackburn, E.H., 2001. Switching and signaling at the telomere. Cell 106, 661–673.
Blasco, M.A., 2005. Telomeres and human disease: aging, cancer and beyond. Nat. Rev. Genet. 6, 611–622.
Chan, C.M., Huang, J.H., Lin, H.H., Chiang, H.S., Chen, B.H., Hong, J.Y., Hung, C.F., 2008. Protective effects of (−)-epigallocatechin gallate on UVA-induced damage in ARPE19 cells. Mol. Vis. 14, 2528–2534.
Chandel, N.S., Vander Heiden, M.G., Thompson, C.B., Schumacker, P.T., 2000. Redox regulation of p53 during hypoxia. Oncogene 19, 3840–3848.
Chin, L., Artandi, S.E., Shen, Q., Tam, A., Lee, S.L., Gottlieb, G.J., Greider, C.W., Depinho, R. A., 1999. p53 deficiency rescues the adverse effects of telomere loss and cooperates with telomere dysfunction to accelerate carcinogenesis. Cell 97, 527–538.
Chyu, K.Y., Babbidge, S.M., Zhao, X., Dandillaya, R., Rietveld, A.G., Yano, J., Dimayuga, P., Cercek, B., Shah, P.K., 2004. Differential effects of green tea-derived catechin on developing versus established atherosclerosis in apolipoprotein E-null mice. Circulation 109, 2448–2453.
Dai, X., Sun, Y., Jiang, Z., 2007. Protective effects of vitamin eagainst oxidative damage induced by abeta(1-40)Cu(II) complexes. Acta Biochim. Biophys. Sin. 39, 123–130.
de Lange, T., 2002. Protection of mammalian telomeres. Oncogene 21, 532–540.
Duan, J., Duan, J., Zhang, Z., Tong, T., 2005. Irreversible cellular senescence induced by prolonged exposure to H_2O_2 involves DNA-damage-and-repair genes and telomere shortening. Int. J. Biochem. Cell Biol. 37, 1407–1420.
Furumoto, K., Inoue, E., Nagao, N., Hiyama, E., Miwa, N., 1998. Age dependent telomere shortening is slowed down by enrichment of intracellular vitamin C via suppression of oxidative stress. Life Sci. 63, 935–948.
Fuster, J.J., Andres, V., 2006. Telomere biology and cardiovascular disease. Circ. Res. 99, 1167–1180.
Gensch, C., Clever, Y.P., Werner, C., Hanhoun, M., Bohm, M., Laufs, U., 2007. The PPAR-gamma agonist pioglitazone increases neoangiogenesis and prevents apoptosis of endothelial progenitor cells. Atherosclerosis 192, 67–74.
Griffith, J.D., Comeau, L., Rosenfield, S., Stansel, R.M., Bianchi, A., Moss, H., de Lange, T., 1999. Mammalian telomeres end in a large duplex loop. Cell 97, 503–514.
Harsdorf, R.V., Li, P.F., Dietz, R., 1999. Signaling pathways in reactive oxygen species-induced cardiomyocyte apoptosis. Circulation 99, 2934–2941.

Henle, E.S., Han, Z., Tang, N., Rai, P., Luo, Y., Linn, S., 1999. Sequence-specific DNA cleavage by Fe^{2+}-mediated fenton reactions has possible biological implications. J. Biol. Chem. 274, 962–971.

Hescheler, J., Meyer, R., Plant, S., Krautwurst, D., Rosenthal, W., Schultz, G., 1991. Morphological, biochemical, and electrophysiological characterization of a clonal cell (H9c2) line from rat heart. Circ. Res. 69, 1476–1486.

Higdon, J.V., Frei, B., 2003. Tea catechins and polyphenols: health effects, metabolism, and antioxidant functions. Crit. Rev. Food Sci. Nutr. 43, 89–143.

Hung, C.F., Huang, T.F., Chiang, H.S., Wu, W.B., 2005. (−)-Epigallocatechin-3-gallate, a polyphenolic compound from green tea, inhibits fibroblast adhesion and migration through multiple mechanisms. J. Cell. Biochem. 96, 183–197.

Hunter, A.L., Choy, J.C., Granville, D.J., 2005. Detection of apoptosis in cardiovascular diseases. Meth. Mol. Med. 112, 277–289.

Johnson, T.M., Yu, Z.X., Ferrans, V.J., Lowenstein, R.A., Finkel, T., 1996. Reactive oxygen species are downstream mediators of p53-dependent apoptosis. Proc. Natl. Acad. Sci. U. S. A. 93, 11848–11852.

Kang, P.M., Izumo, S., 2000. Apoptosis and heart failure—a critical review of the literature. Circ. Res. 86, 1107–1113.

Kemp, T.J., Causton, H.C., Clerk, A., 2003. Changes in gene expression induced by H_2O_2 in cardiac myocytes. Biochem. Biophys. Res. Commun. 307, 416–421.

L'Ecuyer, T., Allebban, Z., Thomas, R., Vander Heide, R., 2004. Glutathione S-transferase overexpression protects against anthracycline-induced H9c2 cell death. Am. J. Physiol. Heart Circ. Physiol. 286, H2057–H2064.

Leri, A., Franco, S., Zacheo, A., Barlucchi, L., Chimenti, S., Limana, F., Nadal-Ginard, B., Kajstura, J., Anersa, P., Blasco, M.A., 2003. Ablation of telomerase and telomere loss leads to cardiac dilatation and heart failure associated with p53 upregulation. EMBO J. 22, 131–139.

Li, Z., Bing, O.H., Long, X., Robinson, K.G., Lakatta, E.G., 1997. Increased cardiomyocyte apoptosis during the transition to heart failure in the spontaneously hypertensive rat. Am. J. Physiol. 272, H2313–H2319.

Mahmoudi, M., Gorenne, I., Mercer, J., Figg, N., Littlewood, T., Bennett, M., 2008. Statins use a novel Nijmegen breakage syndrome-1-dependent pathway to accelerate DNA repair in vascular smooth muscle cells. Circ. Res. 103, 717–725.

McEachern, M.J., Krauskopf, A., Blackburn, E.H., 2000. Telomeres and their control. Annu. Rev. Genet. 34, 331–358.

Multani, A.S., Ozen, M., Narayan, S., Kumar, V., Chandra, J., McConkey, D.J., Newman, R.A., Pathak, S., 2000. Caspase-dependent apoptosis induced by telomere cleavage and TRF2 loss. Neoplasia 2, 339–345.

Ogata, Y., Takahashi, M., Ueno, S., Takeuchi, K., Okada, T., Mano, H., Ookawara, S., Ozawa, K., Berk, B.C., Ikeda, U., Shimada, K., Kobayashi, E., 2003. Antiapoptotic effect of endothelin-1 in rat cardiomyocytes in vitro. Hypertension 41, 1156–1163.

Oh, H., Wang, S.C., Prahash, A., Sano, M., Moravec, C.S., Michael, L.H., Youker, K.A., Entman, M.L., Schneider, M.D., 2003. Telomere attrition and Chk2 activation in human heart failure. Proc. Natl. Acad. Sci. U. S. A. 100, 5378–5383.

Oikawa, S., Kawanishi, S., 1999. Site-specific DNA damage at GGG sequence by oxidative stress may accelerate telomere shortening. FEBS Lett. 453, 365–368.

Peter, M.E., Heufelder, A.E., Hengartner, M.O., 1997. Advances in apoptosis research. Proc. Natl. Acad. Sci. U. S. A. 94, 12736–12737.

Planavila, A., Rodríguez-Calvo, R., Jové, M., Michalik, L., Wahli, W., Laguna, J.C., Vázquez-Carrera, M., 2005. Peroxisome proliferator-activated receptor β/δ activation inhibits hypertrophy in neonatal rat cardiomyocytes. Cardiovasc. Res. 65, 832–841.

Priyadarshi, S., Valentine, B., Han, C., Fedorova, O.V., Bagrov, A.Y., Liu, J., Periyasamy, S.M., Kennedy, D., Malhotra, D., Xie, Z., Shapiro, J.I., 2003. Effect of green tea extract on cardiac hypertrophy following 5/6 nephrectomy in the rat. Kidney Int. 63, 1785–1790.

Ren, J.G., Xia, H.L., Just, T., Dai, Y.R., 2001. Hydroxyl radical-induced apoptosis in human tumor cells is associated with telomere shortening but not telomerase inhibition and caspase activation. FEBS Lett. 488, 123–132.

Rice-Evans, C., 1999. Implications of the mechanisms of action of tea polyphenols as antioxidants in vitro for chemoprevention in humans. Proc. Soc. Exp. Biol. Med. 220, 262–266.

Sano, M., Minamino, T., Toko, H., Miyauchi, H., Orimo, M., Qin, Y., Akazawa, H., Tateno, K., Kayama, Y., Harada, M., Shimizu, I., Asahara, T., Hamada, H., Tomita, S., Molkentin, J.D., Zou, Y., Komuro, I., 2007. p53-induced inhibition of Hif-1 causes cardiac dysfunction during pressure overload. Nature 446, 444–448.

Sheng, R., Gu, Z.L., Xie, M.L., Guo, C.Y., Zhou, W.X., 2007. EGCG inhibits cardiomyocyte apoptosis in pressure overload induced cardiac hypertrophy rats and protects cardiomyocyte from oxidative stress. Acta Pharmacol. Sin. 28, 191–201.

Sheng, R., Gu, Z.L., Xie, M.L., Guo, C.Y., Zhou, W.X., 2009. EGCG inhibits proliferation of cardiac fibroblasts in the rats with cardiac hypertrophy. Planta Med. 75, 113–120.

Spyridopoulos, I., Haendeler, J., Urbich, C., Brummendorf, T.H., Oh, H., Schneider, M.D., Zeiher, A.M., Dimmeler, S., 2004. Statins enhance migratory capacity by upregulation of the telomere repeat-binding factor TRF2 in endothelial progenitor cells. Circulation 110, 3136–3142.

Suh, K.S., Chon, S., Oh, S., Kim, S.W., Kim, J.W., Kim, Y.S., Woo, J.T., 2010. Prooxidative effects of green tea polyphenol (-)-epigallocatethin-3-gallate on the HIT-T15 pancreatic beta cell line. Cell Biol. Toxicol. 26, 189–199.

Townsend, P.A., Scarabelli, T.M., Pasini, E., Gitti, G., Menegazzi, M., Suzuki, H., Knight, R. A., Latchman, D.S., Stephanou, A., 2004. Epigallocatechin-3-gallate inhibits STAT-1 activation and protects cardiac myocytes from ischemia/reperfusion-induced apoptosis. FASEB J. 18, 1621–1623.

Trinei, M., Giorgio, M., Cicalese, A., Barozzi, S., Ventura, A., Migliaccio, E., Milia, E., Padura, I.M., Raker, V.A., Maccarana, M., Petronilli, V., Minucci, S., Bernardi, P., Lanfrancone, L., Pelicci, P.G., 2002. A p53-p66Shc signaling pathway controls intracellular redox status, levels of oxidation-damaged DNA and oxidative stress-induced apoptosis. Oncogene 21, 3872–3878.

van Empel, V.P., Bertrand, A.T., Hofstra, L., Crijns, H.J., Doevendans, P.A., De Windt, L.J., 2005. Myocyte apoptosis in heart failure. Cardiovasc. Res. 67, 21–29.

van Steensel, B., Smogorzewska, A., de Lange, T., 1998. TRF2 protects human telomeres from end-to-end fusions. Cell 92, 401–413.

Voghel, G., Thorin-Trescases, N., Farhat, N., Mamarbachi, A.M., Villeneuve, L., Fortier, A., Perrault, L.P., Carrier, M., Thorin, E., 2008. Chronic treatment with N-acetyl-cystein delays cellular senescence in endothelial cells isolated from a subgroup of atherosclerotic patients. Mech. Ageing Dev. 129, 261–270.

Wencker, D., Chandra, M., Nguyen, K., Miao, W., Garantziotis, S., Factor, S.M., Shirani, J., Armstrong, R.C., Kitsis, R.N., 2003. A mechanistic role for cardiac myocyte apoptosis in heart failure. J. Clin. Invest. 111, 1497–1504.

Werner, C., Hanhoun, M., Widmann, T., Kazakov, A., Semenov, A., Poss, J., Bauersachs, J., Thum, T., Pfreundschuh, M., Muller, P., Haendeler, J., Bohm, M., Laufs, U., 2008. Effects of physical exercise on myocardial telomere-regulating proteins, survival pathways, and apoptosis. J. Am. Coll. Cardiol. 52, 470–482.

Winstead, M.V., Lucas, K.K., Dennis, E.A., 2005. Group IV cytosolic phospholipase A_2 mediates arachidonic acid release in H9c2 rat cardiomyocyte cells in response to hydrogen peroxide. Prostaglandins Other Lipid Mediat. 78, 55–66.

Wu, W.B., Chiang, H.S., Fang, J.Y., Chen, S.K., Huang, C.C., Hung, C.F., 2006. (+)-Catechin prevents ultraviolet B-induced human keratinocyte death via inhibition of JNK phosphorylation. Life Sci. 79, 801–807.

Yao, K., Ye, P., Zhang, L., Tan, J., Tang, X., Zhang, Y., 2008. Epigallocatechin gallate protects against oxidative stress-induced mitochondria-dependent apoptosis in human lens epithelial cells. Mol. Vis. 14, 217–223.